CHAPTER V
CATALYTIC OXIDATION OF VOLATILE ORGANIC COMPOUNDS OVER TRANSITION METAL OXIDE-DOPED CeO_2-ZrO_2 CATALYSTS

5.1 Abstract

In this study, the vapor phase catalytic oxidation of benzene, toluene and naphthalene was studied over $Ce_{0.75}Zr_{0.25}O_2$ and $Ce_{0.75}Zr_{0.15}Me_{0.10}O_2$ (Me = Cr, Fe, Mn and V) mixed oxide catalysts prepared via urea hydrolysis. The results showed that the introduction of transition metal oxides into the CeO_2-ZrO_2 lattice leads to improvement of their redox behaviours, as a consequence, the catalytic activity in VOCs oxidation is enhanced. The $Ce_{0.75}Zr_{0.15}Mn_{0.10}O_2$ solid solution catalyst exhibits the highest activity for the three studied VOCs oxidation, whereas the addition of chromium oxide lowered catalytic activity. By employing the power law model assuming pseudo first order kinetics, the apparent activation energies of benzene, toluene and naphthalene oxidation over $Ce_{0.75}Zr_{0.25}O_2$ and $Ce_{0.75}Zr_{0.15}Me_{0.10}O_2$ (Me = Cr, Fe, Mn and V) mixed oxide catalysts which are calculated from the Arrhenius plot are in the range of 112-225, 92-117 and 68-116 kJ mol^{-1} for benzene, toluene and naphthalene oxidations, respectively.

5.2 Introduction

Volatile organic compounds (VOCs) are a primary air pollutant and have relatively high vapor pressure and thus easily vaporize under ambient conditions. VOCs are known to cause air pollution such as photochemical smog, ground-level ozone, sick house syndrome, and chemical sensitivity (Atkinson *et al.*, 2003). Various methods such as low-temperature condensation, biochemical methods, adsorption-based techniques, and so on, have been intensively investigaed for effective abatement of VOCs (Hester *et al.*, 1995). Catalytic oxidation of VOCs to more environmentally benign CO_2 and H_2O is one of the most effective processes, since it can be operated with dilute VOCs effluent stream and at much lower temperatures than conventional thermal incineration which is required high

temperatures exceeding 1073-1473 K to achieve complete VOCs destruction (Hutchings *et al.*, 1996). Precious metal catalysts, especially supported platinum and palladium catalysts, have been demonstrated as the most active catalysts for destruction of these obnoxious compounds, but the high price and low availability limit their application (Papaefthimiou *et al.*, 1997; Blanco *et al.*, 2007). Alternatively, metal oxide catalysts such as CoO_x, CrO_x, FeO_x, MnO_x, ZnO, TiO_2, CeO_2, V_2O_5-WO_3-TiO_2 as well as perovskite-type oxides were employed for such an application (Finocchio *et al.*, 2000; García *et al.*, 2006; Cellier *et al.*, 2006; Levasseur *et al.*, 2009). Additionally, it was recently reported that metal oxides are not necessarily less active than precious metals (Morales *et al.*, 2006).

Since, the potential effectiveness of catalytic oxidation as a VOCs abatement technique and the search for more active and cost-effective catalysts based on metal oxides for VOCs destruction remains essential, therefore many efforts were directed towards the design and/or improvement of catalytic materials based on metal oxides as a replacement for precious metal catalysts for the total oxidation of VOCs. Among a wide range of metal oxides, CeO_2-based catalysts, in particular CeO_2-ZrO_2 mixed oxides, are attractive due to their widespread applications in many fields. Particularly, these materials are used as the promoter in the three-way catalysts (TWC), catalyst support towards carbon deposition resistance for partial oxidation and reforming reactions and catalysts for oxidation of various hydrocarbons including VOCs, which is due to theirs high oxygen storage capacity and redox properties (Pengpanich *et al.*, 2004; García *et al.*, 2006). It was reported that modifying CeO_x-ZrO_x with other metal oxides, for instance by the partial substitution of trivalent cations, such as Cu, Fe and Mn, into the lattice of CeO_x-ZrO_x solid solution, can improve the oxygen storage capacity and redox properties of CeO_x-ZrO_x mixed oxides, resulting in enhancing the activities in VOCs elimination (Jia *et al.*, 2008; Hu 2009; Nedyalkova *et al.*, 2009).

The aim of this work is to investigate the effect of doping transition metal oxide, in particular Cr, Fe, Mn and V, on the oxidation catalytic activity of benzene, toluene and naphthalene as the VOCs model compounds over $Ce_{0.75}Zr_{0.15}Me_{0.10}O_2$ (Me = Cr, Fe, Mn and V) mixed oxide catalysts.

5.3 Experimental

5.3.1 Catalyst Preparation and Characterizations

A series of mixed oxide samples $Ce_{0.75}Zr_{0.25}O_2$ and $Ce_{0.75}Zr_{0.15}Me_{0.10}O_2$ (Me = Cr, Fe, Mn and V) were prepared via urea hydrolysis. $Ce(NO_3)_3{\cdot}6H_2O$, $ZrOCl_2{\cdot}8H_2O$, $Cr(NO_3)_3{\cdot}9H_2O$, $Fe(NO_3)_3{\cdot}9H_2O$, $Mn(NO_3)_2{\cdot}4H_2O$ and NH_4VO_3 were used as sources of Ce, Zr,Cr, Fe, Mn and V, respectively. The synthesis procedure of catalysts has been reported elsewhere (Pengpanich *et al.*, 2002).

The crystalline structure of the synthesized samples was determined by X-ray diffraction (XRD) on a Rigaku X-ray diffractometer equipped with a RINT 2000 wide-angle goniometer using Cu Kα radiation, 40 kV and 40 mA, in the range 2θ from 20 to 90°.

The textural characteristics, such as BET surface area, pore volume and average pore diameter, were determined by N_2 adsorption-desorption at 77 K in a Micromeritics ASAP 2020 Analyzer. Prior to the analysis, the sample was outgassed to eliminate volatile adsorbents on the surface at 523 K for 24 h.

Hydrogen temperature-programmed reduction (H_2-TPR) experiments were carried out with TPR analyzer (Quantachrome modeled ChemBET-3000 TPR/TPD) using 50 mg· of sample. TPR profiles were attained by heating the samples under a 5% H_2/N_2 flow (75 ml min^{-1}) from 30 K to 900 K at a linearly programmed rate of 10 K min^{-1}.

5.3.2 Activity Tests

Catalytic activity tests for the VOCs oxidation were carried out in a differential fixed-bed quartz tube reactor in which its dimensions were reported elsewhere (Pengpanich *et al.*, 2002). Typically, 50 mg of a catalyst was packed between the layers of quartz wool. The catalyst bed temperature was monitored and controlled by a Shinko temperature controller equipped with two type-K thermocouples inserted at the catalyst bed and next to the reactor. A total flow rate of 200 ml min^{-1} gas mixtures containing 2000 ppm of benzene (or 2000 ppm of toluene

or 200 ppm of naphthalene), 10% oxygen and balance of helium was used. Exit gases were chromatographically analyzed for CO, CO_2 and hydrocarbons using a Shimadzu GC 8A equipped with a TCD detector and a Shimadzu GC 17A equipped with an FID detector.

5.4 Results and Discussion

5.4.1 Catalyst Characterizations

The XRD patterns of the $Ce_{0.75}Zr_{0.25}O_2$ and $Ce_{0.75}Zr_{0.15}Me_{0.10}O_2$ mixed oxide catalysts are presented in Figure. 5.1. All ceria-based materials, except $Ce_{0.75}Zr_{0.15}V_{0.10}O_2$, exhibited basal reflections corresponding to the fluorite type structure of CeO_2, the XRD patterns show visible tailing at about 29°, 33°, 48°, 56° and 60° (2θ), which represent the indices of (1 1 1), (2 0 0), (2 2 0), (3 1 1) and (2 2 2) planes, respectively. For V-containing catalyst, the tiny peak at 2θ about 24° was observed and can be attributed to the formation of a $CeVO_4$ phase (Duarte de Farias *et al.*, 2008). These results are in agreement with the FT-Raman results (Figure 5.2), which are presented only the adsorption peak ca. 460 cm^{-1} for Fe- and Mn-containing catalysts, indicating a typical of the F_{2g} Raman active mode of the fluorite-structured materials (Fornasiero *et al.*, 1996). On the other hand, the Raman spectrum for $Ce_{0.75}Zr_{0.15}Cr_{0.10}O_2$ shows the band at about 860 cm^{-1}, indicating the chromium oxide exists on the surface of mixed oxides (Yim *et al.*, 2004). While band at about 850 cm^{-1} was observed for $Ce_{0.75}Zr_{0.15}V_{0.10}O_2$ sample, indicating the characteristic of $CeVO_4$ phase. Based on the XRD and FT-Raman observation, it appears that all iron, manganese and zirconium cations dissolve in the ceria lattice. The results are similar to those reported elsewhere for Fe- and Mn-CeO_2 mixed oxides (Pérez-Alonso *et al.*, 2005; Machida *et al.*, 2000). This might be because the ionic radii of Fe^{3+} (6.5 nm), Mn^{3+} (6.2 nm) and Zr^{4+} (8.4 nm) are smaller than that of Ce^{4+} (9.7 nm), therefore, dissolution in the ceria lattice would be possible at low doping concentrations for Fe, Mn and Zr.

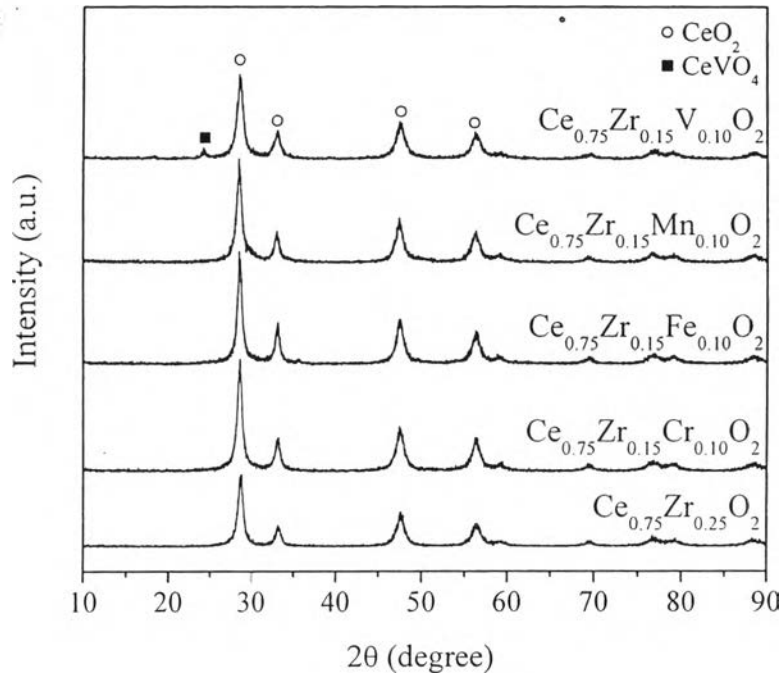

Figure 5.1 X-ray diffraction patterns for $Ce_{0.75}Zr_{0.25}O_2$ and $Ce_{0.75}Zr_{0.15}Me_{0.10}O_2$ (Me = Cr, Fe, Mn and V) mixed oxide catalysts with aging time of 50 h, and calcined at 773 K.

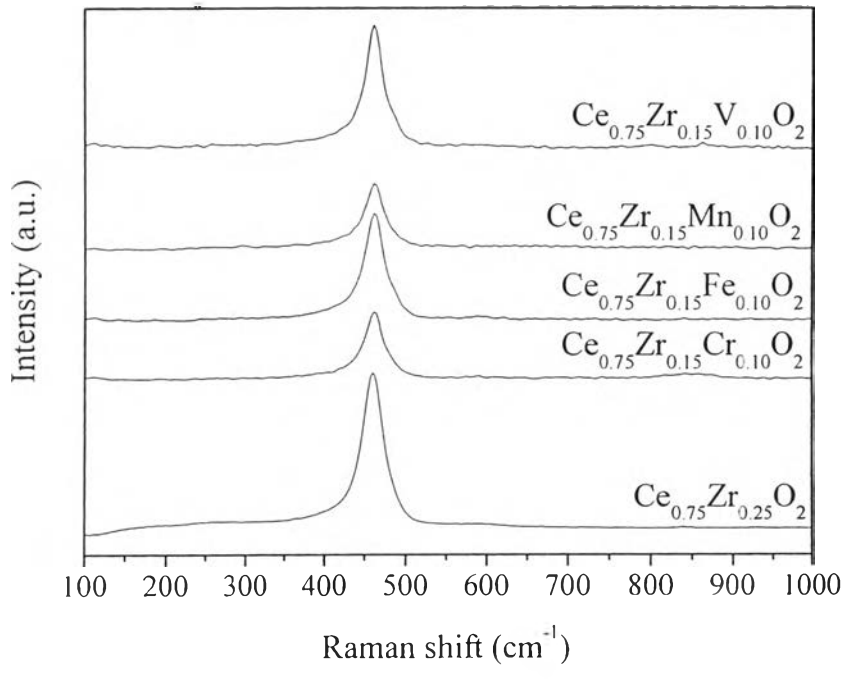

Figure 5.2 Raman spectrum of the $Ce_{0.75}Zr_{0.25}O_2$ and $Ce_{0.75}Zr_{0.15}Me_{0.10}O_2$ (Me = Cr, Fe, Mn and V) mixed oxide catalysts.

Table 5.1 summarizes the BET surface areas, pore volumes and average pore diameters of the mixed oxide catalysts. It can be seen that the BET surface areas of mixed oxide samples are in the range of 102-125 $m^2 g^{-1}$ and the average pore diameters of these mixed oxides are about 3.0-7.1 nm. The BET surface area were slightly increased after incorporation of chromium, manganese and iron, while the surface area of vanadium-doped sample was decreased. This might be because the present of the $CeVO_4$ phase.

Table 5.1 Textural properties of the catalysts

Catalyst	BET surface area ($m^2 g^{-1}$)	Total pore volume ($cm^3 g^{-1}$)	Average pore diameter (nm)
$Ce_{0.75}Zr_{0.25}O_2$	106	0.11	4.0
$Ce_{0.75}Zr_{0.15}Cr_{0.10}O_2$	120	0.10	3.0
$Ce_{0.75}Zr_{0.15}Fe_{0.10}O_2$	111	0.10	3.5
$Ce_{0.75}Zr_{0.15}Mn_{0.10}O_2$	125	0.11	3.4
$Ce_{0.75}Zr_{0.15}V_{0.10}O_2$	102	0.18	7.1

The H_2-TPR profiles of $Ce_{0.75}Zr_{0.25}O_2$ and $Ce_{0.75}Zr_{0.15}Me_{0.10}O_2$ (Me = Cr, Fe, Mn and V) samples are showed in Figure 5.3. It can be seen that $Ce_{0.75}Zr_{0.25}O_2$ exhibits distinct peaks showing maxima at about 843 and 1153 K. The former peak in the low temperature region was the reduction of surface capping oxygen and the latter peak was the reduction of bulk oxygen species (Pengpanich *et al.*, 2004). For Cr-doped catalyst, the reduction peaks at about 673, 763 and 1153 K can be observed, which were assigned to the reduction of Cr-species (Yim *et al.*, 2004), surface and bulk oxygen of cerium oxide, respectively. On the Fe-doped CeO_2-ZrO_2 sample four reduction peaks are observed. The reduction peaks at about 753 K and 943 K can be associated with the reduction of Fe_2O_3 to Fe_3O_4 and Fe_3O_4 to FeO, respectively (Scirè *et al.*, 2008). While the reduction peaks at about 838 and 1173 K were ascribed to the reduction of surface and bulk oxygen of cerium oxide, respectively. For the $Ce_{0.75}Zr_{0.15}Mn_{0.10}O_2$ mixed oxide, the TPR profile of this sample also exhibited two peaks similar to those of $Ce_{0.75}Zr_{0.25}O_2$, which were assigned to the reduction of surface (ca. 783 K) and bulk (ca. 1153 K) oxygen of cerium oxide, respectively. This implies that all manganese cations have dissolved in the ceria lattice to form solid solution, resulting in slightly decreases the reduction temperature of CeO_2-ZrO_2 mixed oxides. For the $Ce_{0.75}Zr_{0.15}V_{0.10}O_2$ mixed oxide sample, the reduction peak at about 1043 K is observed. This corresponds to the removal of oxygen from the bulk of $CeVO_4$, resulting the reduction of V^{5+} (Yasyerli *et al.*, 2006). Among them, the $Ce_{0.75}Zr_{0.15}Cr_{0.10}O_2$ mixed oxides is most reducible, while the non-modified $Ce_{0.75}Zr_{0.25}O_2$ sample shows least reducible. Therefore, we can claim that the incorporation of transition metals, i.e. Cr, Fe, Mn and V, into CeO_2-ZrO_2 improves the reducibility of the mixed oxides.

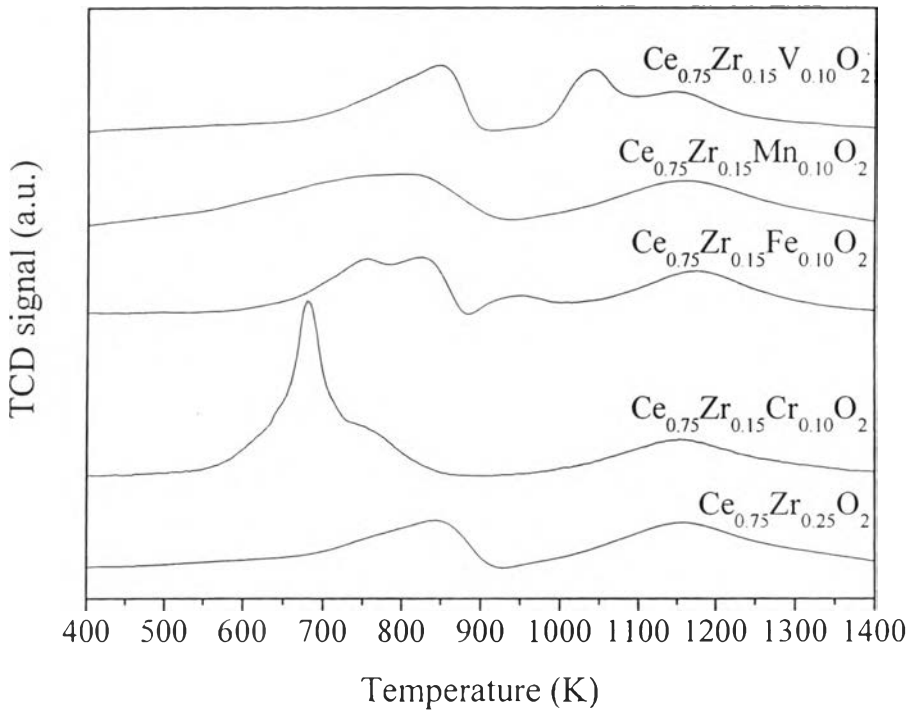

Figure 5.3 H_2-TPR profiles of the $Ce_{0.75}Zr_{0.25}O_2$ and $Ce_{0.75}Zr_{0.15}Me_{0.10}O_2$ (Me = Cr, Fe, Mn and V) mixed oxide catalysts calcined at 773 K with heating rate of 10 K min^{-1}, a reducing gas containing 5% H_2 in nitrogen with a flow rate of 75 ml min^{-1}.

Table 5.2 The amount of H_2 consumption determined from the reduction peak of $Ce_{0.75}Zr_{0.25}O_2$ and $Ce_{0.75}Zr_{0.15}Me_{0.10}O_2$ (Me = Cr, Fe, Mn and V) mixed oxides in TPR profiles shown in Figure 5.3

Catalyst	H_2 consumption ($\mu mol\ g_{cat}^{-1}$)
$Ce_{0.75}Zr_{0.25}O_2$	1374
$Ce_{0.75}Zr_{0.15}Cr_{0.10}O_2$	1643
$Ce_{0.75}Zr_{0.15}Fe_{0.10}O_2$	1393
$Ce_{0.75}Zr_{0.15}Mn_{0.10}O_2$	1791
$Ce_{0.75}Zr_{0.15}V_{0.10}O_2$	1484

5.4.2 Catalytic Activities for VOCs Oxidation

The catalytic activities of $Ce_{0.75}Zr_{0.25}O_2$ and $Ce_{0.75}Zr_{0.15}Me_{0.10}O_2$ (Me = Cr, Fe, Mn and V) mixed oxide for benzene, toluene and naphthalene total oxidation determined in the temperature range of 373-773 K are shown in Figures 5.4-5.6 and Table 5.3. A higher activity is indicated by a lower temperature for 50% conversion of VOCs ($T_{50\%}$). Regardless of the mixed oxide used, CO_2 and H_2O are the only products observed.

Figure 5.4 shows the light-off temperatures for benzene oxidation over $Ce_{0.75}Zr_{0.25}O_2$ and $Ce_{0.75}Zr_{0.15}Me_{0.10}O_2$ (Me = Cr, Fe, Mn and V) mixed oxide catalysts. It was found that $Ce_{0.75}Zr_{0.15}Mn_{0.10}O_2$ was found to exhibit the highest activity for the oxidation of benzene, while Cr-doped CeO_2-ZrO_2 was the least active catalyst. The $T_{50\%}$ value and the temperature for complete benzene oxidation over $Ce_{0.75}Zr_{0.15}Mn_{0.10}O_2$ take place at 555 and 633 K, respectively. On the other hand, the non-modified CeO_2-ZrO_2 catalyst is required the temperature of 673 K for complete benzene destruction. A difference of around 50 K was observed between the $Ce_{0.75}Zr_{0.15}Mn_{0.10}O_2$ and the $Ce_{0.75}Zr_{0.25}O_2$ catalysts at 50% conversion and this difference reaches to 75 K at 100% conversion on the same catalysts. The order of catalytic activity observed is $Ce_{0.75}Zr_{0.15}Mn_{0.10}O_2$ > $Ce_{0.75}Zr_{0.15}Fe_{0.10}O_2$ > $Ce_{0.75}Zr_{0.15}V_{0.10}O_2$ > $Ce_{0.75}Zr_{0.25}O_2$ > $Ce_{0.75}Zr_{0.15}Cr_{0.10}O_2$. The conversion of toluene

over mixed oxide catalysts as a function of reaction temperature is shown in Figure 5.5. It was found that the catalyst ranking is identical to the one found in benzene oxidation, which is $Ce_{0.75}Zr_{0.15}Mn_{0.10}O_2$ mixed oxides appeared to be the most active catalyst presenting $T_{50\%}$ at about 536 K. The doping of chromium oxide aws also found to induce a decrease in oxidation activity. The total toluene oxidation was observed to be complete at 733 K on $Ce_{0.75}Zr_{0.15}Cr_{0.10}O_2$ catalyst in comparision with 673 K on $Ce_{0.75}Zr_{0.25}O_2$ catalyst. In the case of naphthalene oxidation (Figure 5.6), the $Ce_{0.75}Zr_{0.15}Mn_{0.10}O_2$ is again the most active among all catalysts achieving complete naphthalene conversion at 573 K. Similar manner for the oxidation of benzene and toluene, the doping of chromium oxide leads to slowdown of the activity of the naphthalene oxidation on Fe-, Mn- and V-doped CeO_2-ZrO_2 catalysts.

Table 5.3 Catalytic activity for benzene, toluene and naphthalene oxidation expressed by $T_{50\%}$

Catalyst	$T_{50\%}$ (K)		
	Benzene	Toluene	Naphthalene
$Ce_{0.75}Zr_{0.25}O_2$	606	551	534
$Ce_{0.75}Zr_{0.15}Cr_{0.10}O_2$	678	591	539
$Ce_{0.75}Zr_{0.15}Fe_{0.10}O_2$	559	542	520
$Ce_{0.75}Zr_{0.15}Mn_{0.10}O_2$	555	536	515
$Ce_{0.75}Zr_{0.15}V_{0.10}O_2$	567	551	526

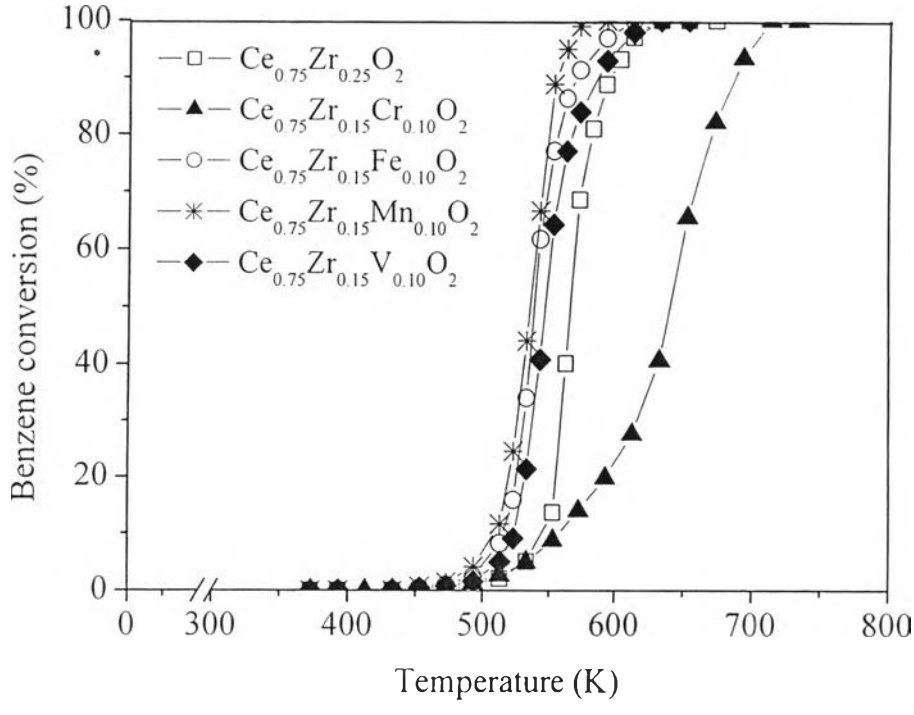

Figure 5.4 Light-off curve for benzene oxidation over $Ce_{0.75}Zr_{0.25}O_2$ and $Ce_{0.75}Zr_{0.15}Me_{0.10}O_2$ (Me = Cr, Fe, Mn and V) mixed oxide catalysts; with gas mixture composed of 2000 ppmv C_6H_6, 10% O_2 and balance He.

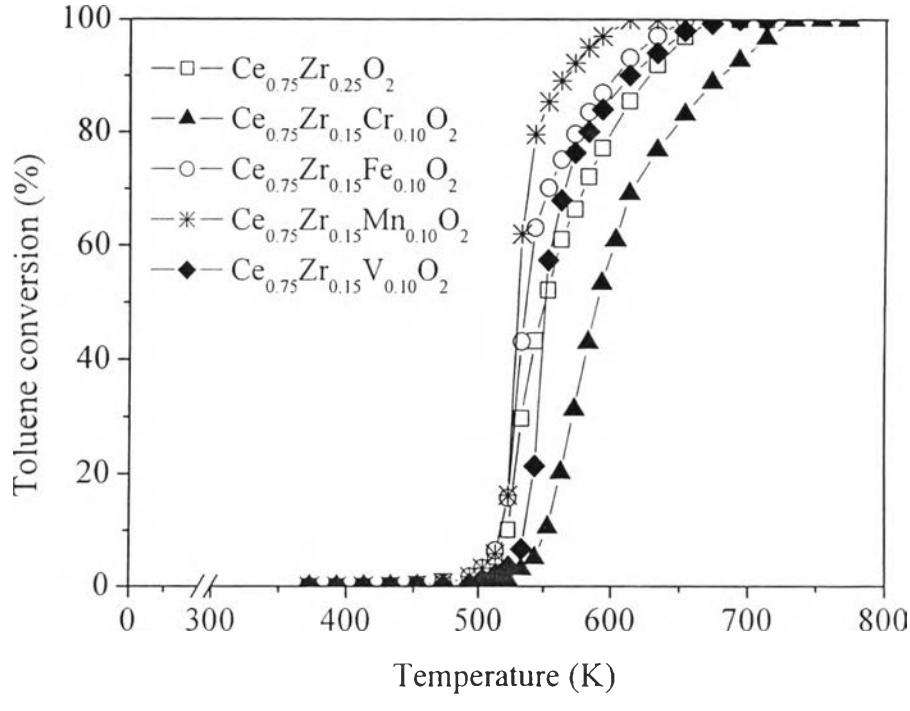

Figure 5.5 Light-off curve for toluene oxidation over $Ce_{0.75}Zr_{0.25}O_2$ and $Ce_{0.75}Zr_{0.15}Me_{0.10}O_2$ (Me = Cr, Fe, Mn and V) mixed oxide catalysts; with gas mixture composed of 2000 ppmv C_7H_8, 10% O_2 and balance He.

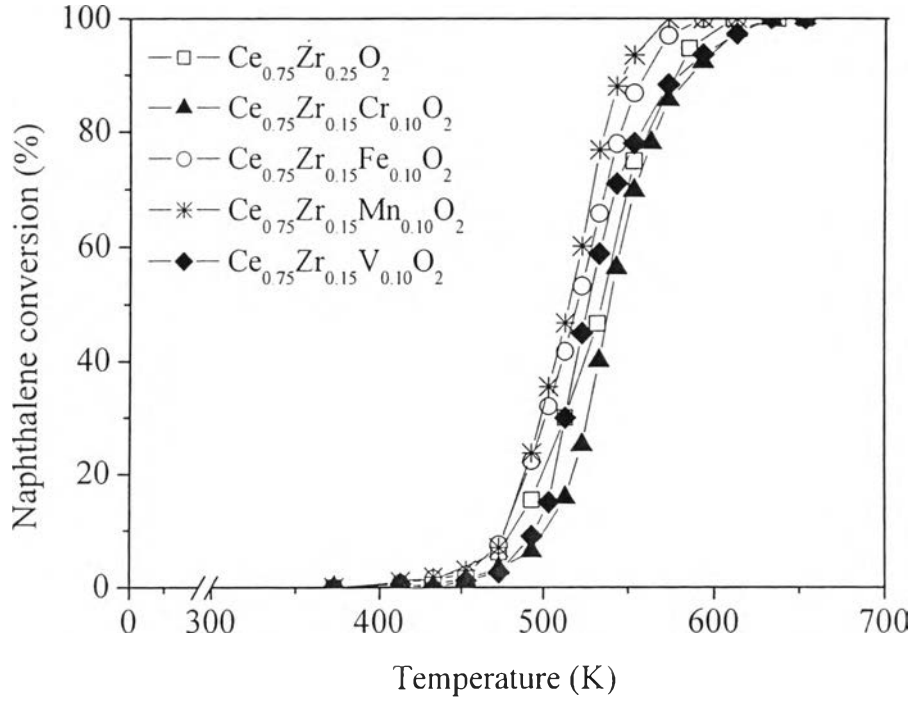

Figure 5.6 Light-off curve for naphthalene oxidation over $Ce_{0.75}Zr_{0.25}O_2$ and $Ce_{0.75}Zr_{0.15}Me_{0.10}O_2$ (Me = Cr, Fe, Mn and V) mixed oxide catalysts; with gas mixture composed of 200 ppmv $C_{10}H_8$, 10% O_2 and balance He.

For all the organic molecules taken into consideration, the correlating $T_{50\%}$ with the nature of the hydrocarbon clearly appears that benzene is the most difficult compound to be oxidized, the shift of $T_{50\%}$ towards larger values being on a range of 16-139 K. The sequence of catalytic activity of the mixed oxide catalysts for the three studied VOCs oxidation follows in the order: $Ce_{0.75}Zr_{0.15}Mn_{0.10}O_2$ > $Ce_{0.75}Zr_{0.15}Fe_{0.10}O_2$ > $Ce_{0.75}Zr_{0.15}V_{0.10}O_2$ > $Ce_{0.75}Zr_{0.25}O_2$ > $Ce_{0.75}Zr_{0.15}Cr_{0.10}O_2$, which is related to the redox properties of the mixed oxide catalysts. However, it should be noted that the most reducible catalyst, namely $Ce_{0.75}Zr_{0.15}Cr_{0.10}O_2$ is the least active among all catalysts for the oxidation of VOCs. It was reported that not only the reducibility of the catalyst, but the strength of bond between adsorbed molecules and catalyst surface was also important parameter affecting aromatic compounds, i.e. naphthalene, catalytic combustion (García *et al.*, 2006; Zhang *et al.*, 2003). The lower activity observed for Cr-doped CeO_2-ZrO_2 catalyst could be presumably related the different interaction between the aromatic substrate and the catalytic surface, considering that aromatic compounds adsorb on the Cr-containing material surface in a higher extent than the other.

The apparent activation energies, E_a, of benzene, toluene and naphthalene oxidation over $Ce_{0.75}Zr_{0.25}O_2$ and $Ce_{0.75}Zr_{0.15}Me_{0.10}O_2$ (Me = Cr, Fe, Mn and V) mixed oxide catalysts were calculated from Arrhenius plots as shown in Table 5.4. For all mixed oxide catalysts the corresponding Arrhenius plots were linear for conversion levels bebelow 30% conversion where diffusional effects are neglectable, suggesting a single kinetic domain. It was found that the apparent activation energies calculated from the plot were in the range of 112-225, 92-117 and 68-116 kJ mol^{-1} for benzene, toluene and naphthalene oxidations, respectively.

In order to verify if the experimental data obey a Cremer–Constable relation (Constable, 1925; Cremer, 1929):

$$\ln A = mE_a + c \qquad (5.1)$$

, the plot of pre-exponential factors, ln A, and apparent activation energies, E_a, of the reactions of benzene, toluene and naphthalene oxidation over $Ce_{0.75}Zr_{0.25}O_2$ and

$Ce_{0.75}Zr_{0.15}Me_{0.10}O_2$ mixed oxide catalysts is presented in Figure 5.7. A linear plot was obtained thereby indicating that a compensation phenomenon took place. It was reported that the slope of Constable plot should be equal to $\sim(RT)^{-1}$, which means that it is independent of reaction mechanism and kinetics (Lynggaard *et al.*, 2004). In the present work, measurements were carried out in the temperature range of 493-653 K. Assuming an average temperature of 300 K, the $(RT)^{-1}$ term is 0.210, which is in good agreement with the experimentally determined slope m, which was determined to be 0.209 mol kJ^{-1}. Similar phenomenon was also observed in the cases of ethanol, ethyl acetate and toluene oxidation over Cu_xCe_{1-x} catalysts (Delimaris *et al.*, 2009). When specific reactions are compared over different catalysts, the nonlinearity is caused by differences in binding energies and activation enthalpies.

Table 5.4 Apparent activation energies of VOCs oxidation

Catalyst	Benzene (kJ mol^{-1})	Toluene (kJ mol^{-1})	Naphthalene (kJ mol^{-1})
$Ce_{0.75}Zr_{0.25}O_2$	225±5	101±3	68±3
$Ce_{0.75}Zr_{0.15}Cr_{0.10}O_2$	112±3	107±3	101±3
$Ce_{0.75}Zr_{0.15}Fe_{0.10}O_2$	172±4	96±3	73±3
$Ce_{0.75}Zr_{0.15}Mn_{0.10}O_2$	170±4	92±2	82±2
$Ce_{0.75}Zr_{0.15}V_{0.10}O_2$	186±5	117±3	116±3

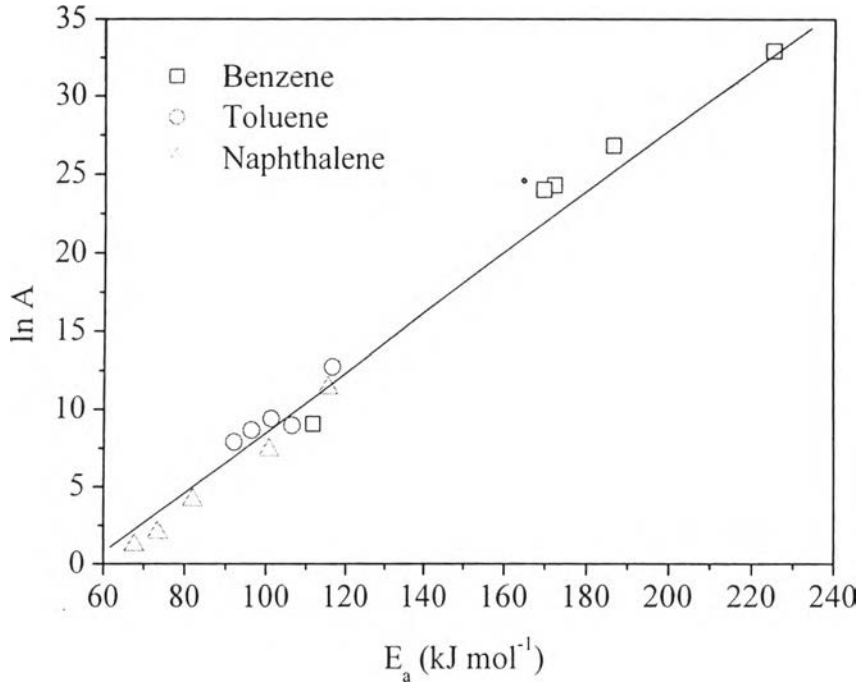

Figure 5.7 Constable plot of pre-exponential factors as a function of apparent activation energies for the catalytic oxidation of VOCs over $Ce_{0.75}Zr_{0.15}Me_{0.10}O_2$ mixed oxide catalysts.

5.5 Conclusions

In conclusion, the incorporation of Cr, Fe, Mn and V cations into CeO_2-ZrO_2 mixed oxide is able to improve the redox properties of CeO_2-ZrO_2 mixed oxides. The Mn-doped CeO_2-ZrO_2 mixed oxides catalyst, $Ce_{0.75}Zr_{0.15}Mn_{0.10}O_2$, was found to exhibits the highest activity toward complete oxidation of the three studied VOCs, appearing to be effective at relatively low temperatures for non-precious catalysts, which is related to the redox properties of the mixed oxide catalysts. Even so, it is not true in the case of Cr-doped where the catalytic activity is not correlated to redox properties. The apparent activation energies of benzene, toluene and naphthalene oxidation over these mixed oxide catalysts are in the range of 112-225,

92-117 and 68-116 kJ mol^{-1} for benzene, toluene and naphthalene oxidations, respectively; assusming pseudo first order kinetics.

5.6 Acknowledgements

This work was supported by the Thailand Research Fund (under Waste-to-Energy project and Royal Golden Jubilee Ph.D. Program: Grant 0170/46), and the Research Unit for Petrochemical and Environmental Catalysts, Ratchadapisek Somphot Endowment Fund, and the National Center of Excellence for Petroleum, Petrochemicals and Advanced Materials, Chulalongkorn University.

5.7 References

Atkinson, R., Arey, J. (2003) Atmospheric degradation of volatile organic compounds. Chemical Reviews, 103, 4605-4638.

Blanco, J., Petre, A.L., Yates, M., Martin, M.P., Martin, J.A., Martin-Luengo, M.A. (2007) Tailor-made high porosity VOC oxidation catalysts prepared by a single-step procedure. Applied Catalysis B: Environmental, 73, 128-134.

Cellier, C., Ruaux, V., Lahousse, C. (2006) Extent of the participation of lattice oxygen from γ-MnO_2 in VOCs total oxidation: Influence of the VOCs nature. Catalysis Today, 117, 350-355.

Constable, F.H. (1925) The Mechanism of Catalytic Decomposition. Proceedings of the Royal Society of London. Sereis A, 108, 355-378.

Cremer, E. (1929) Das katalytische Verhalten der Oxide seltener Erden. Zeitschrift für Physikalische Chemie, 144, 231-242.

Delimaris, D., Ioannides, T. (2009) VOC oxidation over CuO–CeO_2 catalysts prepared by a combustion method. Applied Catalysis B: Environmental, 89, 295-302.

Duarte de Farias, A.M., Bargiela, P., Rocha, M.G., Fraga, M. (2008) Vanadium-promoted Pt/CeO_2 catalyst for water-gas shift reaction. Journal of Catalysis, 260, 93-102.

Finocchio, E., Baldi, M., Busca, G., Pistarino, C., Romezzano, G., Bregani, F., Toledo, C.P. (2000) A study of the abatement of VOC over V_2O_5–WO_3–TiO_2 and alternative SCR catalysts. Catalysis Today, 59, 261-268.

Fornasiero, P., Balducci, G., Monte, R.D., Kaspar, J., Sergo, V., Gubitosa, G., Ferrero, A., Graziani, M. (1996) Modification of the redox behaviour of CeO_2 induced by structural doping with ZrO_2. Journal of Catalysis, 164, 173-183.

García, T.,Solsona, B., Taylor, S.H. (2006) Naphthalene total oxidation over metal oxide catalysts. Applied Catalysis B: Environmental, 66, 92-99.

Hester, R.E., Harrison, R.M. (1995) Volatile Organic Compounds in the Atmosphere, The RSC Cambridge.

Hu, C. (2009) Highly efficient complete oxidation of dilute benzene over ultrafine $Cu_{0.1}Ce_{0.5}Zr_{0.4}O_{2-\delta}$ catalyst in a fluidized bed reactor. Catalysis Communications, 10, 2008-2012.

Hutchings, G.J., Heneghan, C.S., Hudson, I.D., Taylor, S.H. (1996) Uranium-oxide-based catalysts for the destruction of volatile chloro-organic compounds. Nature, 384, 341-343.

Jia, L., Shen, M., Hao, J., Rao, T., Wang, J. (2008) Dynamic oxygen storage and release over $Mn_{0.1}Ce_{0.9}O_x$ and $Mn_{0.1}Ce_{0.6}Zr_{0.3}O_x$ complex compounds and structural characterization. Journal of Alloys and Compounds, 454, 321-326.

Levasseur, B., Kaliaguine, S. (2009) Effects of iron and cerium in La1-yCeyCo1-xFexO3 perovskites as catalysts for VOC oxidation. Applied Catalysis B: Environmental, 88, 305-314.

Lynggaard, H., Andreasen, A., Stegelmann, C., Stoltze, P. (2004) Analysis of simple kinetic models in heterogeneous catalysis. Progress in Surface Science, 77, 71-137.

Machida, M., Uto, M., Kurogi, D., Kijima, T. (2000) MnO_x–CeO_2 Binary Oxides for Catalytic NO_x Sorption at Low Temperatures. Sorptive Removal of NO_x. Chemistry of Materials, 12, 3158-3164.

Morales, M.R., Barbero, B.P., Cadús, L.E. (2006) Total oxidation of ethanol and propane over Mn-Cu mixed oxide catalysts. Applied Catalysis B: Environmental, 67, 229-236.

Nedyalkova, R., Niznansky, D., Roger, A.-C. (2009) Iron–ceria–zirconia fluorite catalysts for methane selective oxidation to formaldehyde. Catalysis Communications, 10, 1875-1880.

Papaefthimiou, P., Ioannides, T., Verykios, X.E. (1997) Combustion of non-halogenated volatile organic compounds over group VIII metal catalysts. Applied Catalysis B: Environmental, 13, 175-184.

Pengpanich, S., Meeyoo, V., Risksomboon, T., Bunyakiat, K. (2002) Catalytic oxidation of methane over CeO_2-ZrO_2 mixed oxide solid solution catalysts prepared via urea hydrolysis. Applied Catalysis A: General, 234, 221-233.

Pengpanich, S., Meeyoo, V., Risksomboon, T. (2004) Methane partial oxidation over Ni/CeO_2–ZrO_2 mixed oxide solid solution catalysts. Catalysis Today, 93-95, 95-105.

Pérez-Alonso, F.J., Granados, M.L., Ojeda, M., Terreros, P., Rojas, S., Herranz, T., Fierro, J.L.G. (2005) Chemical Structures of Coprecipitated Fe–Ce Mixed Oxides. Chemistry of Materials, 17, 2329-2339.

Scirè, S., Crisafulli, C., Minicò, S., Condorelli, G.G., Mauro, A.D. (2008) Selective oxidation of CO in H_2-rich stream over gold/iron oxide: An insight on the effect of catalyst pretreatment. Journal of Molecular Catalysis A: Chemical, 284, 24-32.

Yasyerli, S., Dogu, G., Dogu, T. (2006) Selective oxidation of H_2S to elemental sulfur over Ce-V mixed oxide and CeO_2 catalysts prepared by the complexation technique. Catalysis Today, 117, 271-278.

Yim, S.D., Nam, I.-S. (2004) Characteristics of chromium oxides supported on TiO_2 and Al_2O_3 for the decomposition of perchloroethylene. Journal of Catalysis, 221, 601-611.

Zhang, X.-W., Chen, S.C., Yu, L.E., Kawi, S., Hidajat, K., Ng, K.Y.S. (2003) Oxidative decomposition of naphthalene by supported metal catalysts. Applied Catalysis A: General, 250, 341-352.